Calhoun: The NPS Institutional Archive

DSpace Repository

Theses and Dissertations | 1. Thesis and Dissertation Collection, all items

1971-09

The formation of hydraulic jumps in a rotating, continuously stratified system.

Kurth, Robert Paul

Monterey, California ; Naval Postgraduate School

http://hdl.handle.net/10945/15726

This publication is a work of the U.S. Government as defined in Title 17, United States Code, Section 101. Copyright protection is not available for this work in the United States.

Downloaded from NPS Archive: Calhoun

http://www.nps.edu/library

Calhoun is the Naval Postgraduate School's public access digital repository for research materials and institutional publications created by the NPS community. Calhoun is named for Professor of Mathematics Guy K. Calhoun, NPS's first appointed -- and published -- scholarly author.

Dudley Knox Library / Naval Postgraduate School
411 Dyer Road / 1 University Circle
Monterey, California USA 93943

THE FORMATION OF HYDRAULIC JUMPS IN A ROTATING, CONTINUOUSLY STRATIFIED SYSTEM

Robert Paul Kurth

United States
Naval Postgraduate School

THESIS

THE FORMATION OF HYDRAULIC JUMPS
IN A ROTATING,
CONTINUOUSLY STRATIFIED SYSTEM

by

Robert Paul Kurth

Co-Thesis Advisors: R. T. Williams
G. J. Haltiner

September 1971

Approved for public release; distribution unlimited.

The Formation of Hydraulic Jumps in a Rotating, Continuously Stratified System

by

Robert Paul Kurth
Lieutenant, United States Navy
B.S.E., Kansas State Teachers College, 1966

Submitted in partial fulfillment of the
requirements for the degree of

MASTER OF SCIENCE IN METEOROLOGY

from the

NAVAL POSTGRADUATE SCHOOL
September 1971

Thesis
K89v
c. 1

ABSTRACT

The formation of hydraulic jumps in a rotating, continuously stratified, Boussinesq fluid is investigated. A scale analysis indicates that jump-formation cases should be separated from non-jump cases by the curve $F = ARo^2$ where Ro and F are the initial Rossby and Froude numbers, respectively. Numerical solutions verify the curve up to $F = 0.3$ and show that A is in the range 6.0 to 7.5. The solutions for $F = 1.0$ are examined in considerable detail. The results of this paper extend the work of Houghton and Williams and Hori.

TABLE OF CONTENTS

I. INTRODUCTION ---------- 6

II. BASIC EQUATIONS ---------- 9

III. FINITE DIFFERENCE APPROXIMATIONS ---------- 13

IV. SCALE ANALYSIS ---------- 16

V. INITIAL CONDITIONS ---------- 19

VI. NUMERICAL SOLUTIONS ---------- 21

VII. CONCLUSIONS ---------- 32

LIST OF REFERENCES ---------- 33

INITIAL DISTRIBUTION LIST ---------- 35

FORM DD 1473 ---------- 38

LIST OF ILLUSTRATIONS

FIGURE		Page
1	Arrangements of variables in z	13
2	The quantity d as a function of DNt/L for F = 1.0 and Ro = ∞. Each curve corresponds to a different value of $\Delta X = 2\pi L/n$	22
3	The fields u', v' and θ' at various times for F = 1.0 and Ro = 1.0	24
4	The fields u', v' and θ' at various times for F = 1.0 and Ro = 0.1	24
5	The fields u', v' and θ' at various times for F = 1.0 and Ro = 0.35	25
6	The fields u', v' and θ' at various times for F = 0.04 and Ro = 0.09	27
7	The fields u', v' and θ' at various times for F = 0.04 and Ro = 0.07	27
8	The fields u', v' and θ' at various times for F = 0.3 and Ro = 0.3	28
9	The fields u', v' and θ' at various times for F = 0.3 and Ro = 0.1	28
10	The lowest five layers of the model at time zero and at approximate jump time for F = 1.0 and Ro = 1.0	29
11	Summary of jump-formation experiments with the logarithm of F plotted against the logarith of Ro. The crosses indicate jump occurrence and the dots indicate cases where no jumps were found	30

ACKNOWLEDGMENTS

The author wishes to express his deep gratitude to Dr. Roger Terry Williams and Dr. George J. Haltiner whose recommendations, counsel, encouragement and infinite patience were great factors in the compilation of this thesis.

The author, furthermore, wishes to thank the W. R. Church Computer Center at the Naval Postgraduate School on whose computer system IBM 360/67 all numerical computations were performed. A special thanks is given to the staff of the Computer Center without whose knowledge and guidance this experiment could never have been completed.

A special thank you is given to Dr. Roger Terry Williams who cheerfully allowed his basic frontogenesis model to be modified for the experiments conducted.

I. INTRODUCTION

The formation of hydraulic jumps has been shown for a one-layer, homogeneous fluid for both non-rotating and rotating cases. This experiment will consider a one-layer, continuously stratified fluid by first investigating jumps in a non-rotating coordinate system and then extending the study to the rotating system.

In a non-rotating one-layer fluid a hydraulic jump with a discontinuity in the velocity can arise from an initial state having any scale. If the system rotates, there may be a limiting initial scale beyond which jumps cannot form as shown by Houghton [1969] and Williams and Hori [1970]. A similar behavior is expected in a continuously stratified atmosphere. In non-dimensional terms this corresponds to a critical Rossby number (Ro - U/fL, where U is the initial velocity scale, L is the initial space scale and f is the Coriolis parameter) below which jumps are excluded. This process also depends on the Froude number ($F = U/[D(g\theta_o^{-1} d\theta_o/dz)^{\frac{1}{2}}]$, where D is the vertical scale and θ_o is the mean potential temperature). In the F-Ro plane there should exist a critical curve that would separate the jump cases from the non-jump cases as has been shown for a homogeneous fluid by Houghton [1969] and Williams and Hori [1970]. In this experiment it was shown that a critical curve exists and is valid for time periods of order $L/[D(g\theta_o^{-1} d\theta_o/dz)^{\frac{1}{2}}]$. For longer time periods, however, jumps

may occur in the non-jump region, indicating that the critical 'curve' is actually a zone where the jump time increases rapidly.

There are several possible applications of this work in meteorology and oceanography. Rotation does have an effect on mesoscale motions in the atmosphere, but the influence is not dominant as it is in large-scale motions. Tepper [1952] has proposed that squall lines are modified hydraulic jumps. Freeman [1948], Abdullah [1966], and Houghton and Kasahara [1968] have proposed other mesoscale hydraulic analogies. Sasaki [1959] and Ogura and Charney [1962] have studied squall lines in continuously stratified atmospheres.

Internal waves in the ocean are affected by rotation, and the breaking of these waves should be described by this model. Rapidly moving frontlike temperature disturbances have been observed in the ocean [Gowans, 1969] and these may be internal waves modified by rotation.

In this experiment the Boussinesq equations are given and the modeling relations are introduced in II. In the model the time-dependent quantities are functions of x and z only. The quantity f is assumed to be constant for each independent case study. The finite difference approximations are presented in III. A scale analysis is presented in IV which is useful in the discussion of the numerical solutions. The initial conditions are given in V and the numerical solutions are presented and discussed in VI. The initial state consists of a sinusoidal disturbance (amplitude dependent on F) which is superimposed on the basic state. After a sufficient period of time, the sine wave is distorted

in such a way that a hydraulic jump is formed. In VII conclusions and recommendations for further investigation are given.

II. BASIC EQUATIONS

In this experiment the Boussinesq equations are employed and the domain is bounded by two rigid horizontal planes. The compressibility of the atmosphere is neglected in the Bossinesq approximation. This should not be of qualitative importance since the density scale height of the atmosphere is much larger than the vertical scale of the typical jump zone. The hydrostatic approximation is also used in this experiment and it should be good as long as the horizontal scale is much larger than the vertical scale [Lamb, 1945, p. 258].

The Boussinesq equations which were obtained by Ogura and Phillips [1962] can be written in the following form when the earth's rotation is included:

$$\frac{\partial \vec{V}}{\partial t} + \nabla\cdot(\vec{V}\vec{V}) + \frac{\partial}{\partial z}(w\vec{V}) + \nabla\phi + f\hat{k}\times\vec{V} = 0, \tag{II. 1}$$

$$\frac{\partial \theta}{\partial t} + \nabla\cdot\theta\vec{V} + \frac{\partial}{\partial z}(w\theta) = 0, \tag{II. 2}$$

$$\nabla\cdot\vec{V} + \frac{\partial w}{\partial z} = 0 \quad \text{and} \tag{II. 3}$$

$$\frac{\partial \phi}{\partial z} = \frac{g\theta}{\theta_o}, \tag{II. 4}$$

where:

θ_o = constant reference potential temperature,

P_o = constant reference pressure,

κ = R/C_p,

θ = $T(P_o/P)^{\kappa} - \theta_o$ = departure of the potential temperature from θ_o, and

ϕ = $C_p\theta_o(P/P_o)^{\kappa} + gz$.

Heating and friction have been neglected in these equations even though they may be important under certain conditions.

All quantities are independent of **y** in this model. The Coriolis parameter, f, is assumed to be constant throughout the model but is varied for individual cases. A Cartesian coordinate system is introduced with x increasing toward the east and y increasing toward the north. The x and y velocity components are u and v respectively.

For this model, Equations (II. 1)-(II. 3) can be written in the following form:

$$\frac{\partial u}{\partial t} + \frac{\partial(uu)}{\partial x} + \frac{\partial(uw)}{\partial z} + \frac{\partial \phi}{\partial x} - fv = 0, \tag{II. 5}$$

$$\frac{\partial v}{\partial t} + \frac{\partial(uv)}{\partial x} + \frac{\partial(vw)}{\partial z} + fu = 0, \tag{II. 6}$$

$$\frac{\partial \theta}{\partial t} + \frac{\partial(u\theta)}{\partial x} + \frac{\partial(w\theta)}{\partial z} = 0 \quad \text{and} \tag{II. 7}$$

$$\frac{\partial u}{\partial x} + \frac{\partial w}{\partial z} = 0. \tag{II. 8}$$

The boundary conditions are

$$w = 0, \quad z = 0, D \tag{II. 9}$$

where D is the distance between the horizontal plates.

The integral of Equation (II. 4) gives the departure of ϕ from its vertical average, and this average can be obtained as follows. The following averages are defined:

$$\overline{(\ )} \equiv \frac{1}{2\pi L} \int_0^{2\pi L} (\ )\, dz, \quad \langle (\ ) \rangle \equiv \frac{1}{D} \int_0^D (\ )\, dz, \tag{II. 10}$$

where $2\pi L$ is the periodicity of the fields in x. If Equation (II. 8) is averaged vertically and (II. 9) employed

$$\frac{\partial \langle u \rangle}{\partial x} = 0 \quad \text{or} \quad \langle u \rangle = \langle (\bar{u}) \rangle. \tag{II. 11}$$

Similarly, the vertical average of (II. 5) is

$$\frac{\partial \langle u \rangle}{\partial t} + \frac{\partial \langle uu \rangle}{\partial x} + \frac{\partial \langle \phi \rangle}{\partial x} - f \langle v \rangle = 0. \tag{II. 12}$$

If this equation is in turn averaged with x and if periodicity in x is imposed, Equation (II. 12) can be written

$$\frac{d \langle (\bar{u}) \rangle}{dt} - f \langle (\bar{v}) \rangle = 0. \tag{II. 13}$$

The quantity $\langle (\bar{v}) \rangle$ represents the net mass flux in the y direction. If $\langle (\bar{v}) \rangle$ were different from zero, $\left\langle \left(\frac{\partial \overline{w}}{\partial z} \right) \right\rangle$ could not be zero if a wall were present at some value of y. Since this would violate the boundary conditions [Equation (II. 9)], the following is a requirement in this experiment:

$$\langle(\bar{v})\rangle = 0. \tag{II. 14}$$

It then follows directly from (II. 13) that

$$\frac{d\langle(\bar{u})\rangle}{dt} = 0. \tag{II. 15}$$

Now from (II. 11) $\frac{\partial\langle u\rangle}{\partial t} = \frac{d\langle(\bar{u})\rangle}{dt}$ which together with (II. 15) reduces (II. 12) to $\frac{\partial\langle\phi\rangle}{\partial x} = -\frac{\partial\langle uu\rangle}{\partial x} + f\langle v\rangle.$ (II. 16)

The corresponding equation is obtained by averaging Equation (II. 6) in x and z and by introducing (II. 14), i. e.,

$$f\langle(\bar{u})\rangle = 0. \tag{II. 17}$$

Equation (II. 17) shows that the x- and z-averaged zonal wind is zero. If Equations (II. 4), (II. 16) and (II. 17) are used, Equations (II. 5) and (II. 6) can be rewritten in the forms

$$\frac{\partial u}{\partial t} + \frac{\partial(uu)}{\partial x} - \frac{\partial\langle uu\rangle}{\partial x} + \frac{\partial(uw)}{\partial z} - f(v - \langle v\rangle) + \frac{\partial}{\partial x}(\phi - \langle\phi\rangle) = 0 \quad \text{and} \tag{II. 18}$$

$$\frac{\partial v}{\partial t} + \frac{\partial(uv)}{\partial x} + \frac{\partial(wv)}{\partial z} + fu = 0. \tag{II. 19}$$

By integrating the hydrostatic equation [Equation (II. 4)] the following expression for $\phi - \langle\phi\rangle$ is obtained:

$$\phi - \langle\phi\rangle = \frac{g}{\theta_0}\left[\int_0^z \theta\, dz - \left\langle\int_0^z \theta\, dz\right\rangle\right]. \tag{II. 20}$$

The following energy integral is an invariant for this model:

$$E = \left[\langle(\overline{u^2})\rangle + \langle(\overline{v^2})\rangle\right]/2 - g\left\langle\left(\frac{\overline{z\theta}}{\theta_0}\right)\right\rangle. \tag{II. 21}$$

III. FINITE DIFFERENCE APPROXIMATIONS

Equations (II. 7), (II. 8), (II. 18) and (II. 19) were solved numerically by introducing finite differences in x, z and t. The solutions were obtained by a simple marching process, but if the horizontal variations were two-dimensional, Poisson's equation would have to be solved at each time step [Smagorinski, 1958; Hinkelmann, 1959].

The vertical domain was divided into 2K layers of equal thickness, and the surfaces separating the layers were denoted by k. The arrangement of variables on the bounding surfaces is shown in Figure 1. The divergence of the vertical flux of the scalar S at $z = z_k$ is approximated as

$$\left[\frac{\partial (wS)}{\partial z}\right]_k = \frac{w_{k+\frac{1}{2}}(S_{k+1} + S_k) - w_{k-\frac{1}{2}}(S_k + S_{k-1})}{2(z_{k+\frac{1}{2}} - z_{k-\frac{1}{2}})} \,. \qquad \text{(III. 1)}$$

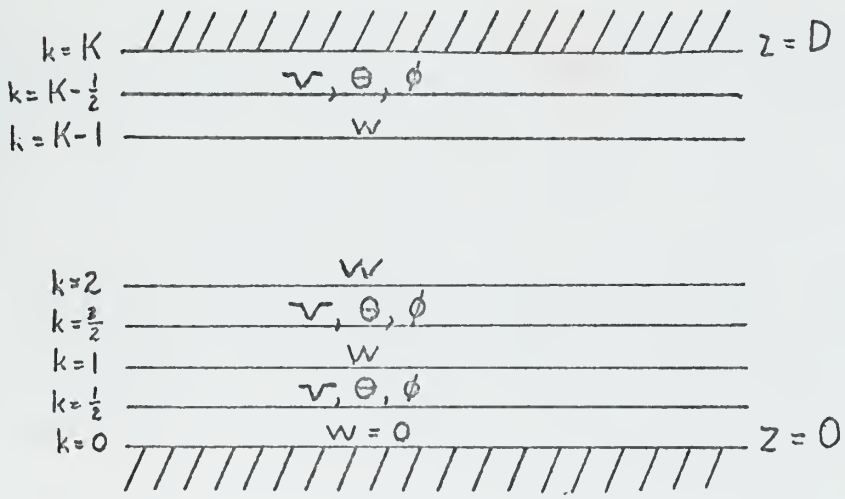

Fig. 1. Arrangement of variables in z.

The finite difference approximation to the integral in Equation (II.20) used is

$$\int_0^{z_k} \theta \, dz = \sum_{j=\frac{1}{2}}^{j=k-\frac{1}{2}} \left[\frac{(\theta_{j+1} + \theta_j)}{2} (z_{j+1} - z_j) \right] + C, \quad k > \tfrac{1}{2}. \tag{III. 2}$$

The value of $C = \int_0^{z_{\frac{1}{2}}} \theta \, dz$ is immaterial since it will disappear when the vertical average is removed. The finite difference integral of Equation (II. 8) used is

$$w_k = -\sum_{j=\frac{1}{2}}^{j=k-\frac{1}{2}} \left[\frac{\partial u_j}{\partial x} (z_{j+\frac{1}{2}} - z_{j-\frac{1}{2}}) \right]. \tag{III. 3}$$

The vertical grid structure was introduced by Lorenz [1960] for use in the balance equations.

All of the dependent variables occur at each x grid point. The x derivatives were approximated as

$$\left(\frac{\partial S}{\partial x} \right)_i = \frac{S_{i+1} - S_{i-1}}{2\Delta x} \quad \text{and} \tag{III. 4}$$

$$\left[\frac{\partial (uS)}{\partial x} \right]_i = \frac{(u_{i+1} + u_i)(S_{i+1} + S_i) - (u_i + u_{i-1})(S_i + S_{i-1})}{4\Delta x}. \tag{III. 5}$$

Here i denotes the grid index and Δx the mesh length. This is a variant of the finite difference scheme that Arakawa [1966] developed [see also Lilly, 1965]. The Arakawa scheme is designed to avoid the non-linear computational instability which was discovered by Phillips [1959]. In particular, the finite difference approximation to the integral,

$$I \equiv \left\langle \left(\overline{\frac{S\,\partial(uS)}{\partial x}} \right) \right\rangle + \left\langle \left(\overline{\frac{S\,\partial(wS)}{\partial z}} \right) \right\rangle , \qquad \text{(III. 6)}$$

is zero when (III. 1) and (III. 5) are used. The integral I is always zero in the continuous case. If the domain averages of u^2, v^2 and θ^2 are conserved by the non-linear terms throughout a numerical integration, then no non-linear computational instability can occur. When finite differences in time are employed, these quantities will not be identically conserved and instability may arise.

The continuous equations conserve the total energy E, which is given by Equation (II. 21). If non-linear computational instability occurs, E cannot be conserved. It was found that E remained nearly constant in the numerical solutions in this experiment, which indicates that the spurious computational production of energy was small. This was important because it was desired that the computational scheme would not introduce a small-scale energy source which could produce a false jump.

Centered time differences were used throughout this experiment with the exception of the first time step which was a forward time step.

IV. SCALE ANALYSIS

A scale analysis is now performed that will indicate the dependence of the solutions on the Rossby number and Froude number. The independent variables are written

$$t = Tt', \quad x = Lx' \text{ and } z = Dz'. \tag{IV.1}$$

The dependent variables are scaled as follows:

$$u = Uu', \quad v = Vv', \quad w = Ww', \quad \emptyset = UDN\emptyset' \text{ and}$$

$$\theta = (UN\theta_o/g)\theta'. \tag{IV.2}$$

The Rossby number and Froude number are defined as

$$Ro = U/fL \text{ and } F = U/DN \tag{IV.3}$$

where N is defined as

$$N = \left[\frac{g}{\theta_o}\frac{\partial\bar{\theta}}{\partial z}\right]^{\frac{1}{2}} \tag{IV.4}$$

The time scale T and the v-scale V are functions of Ro and F while the w-scale is W = UD/L.

An examination of the case where $F \lesssim 1$ and $F \lesssim Ro$ is now given. This should parallel the results obtained by Houghton [1969]. The appropriate time scale is T = L/DN, and the v-scale is V = (F/Ro)U. The later was obtained following Houghton by balancing $\frac{\partial v}{\partial t}$ with fu in Equation (II.6). The non-dimensional equations for this case are

$$\frac{\partial u'}{\partial t'} + F\left[\frac{\partial(u'u')}{\partial x'} + \frac{\partial(u'w')}{\partial z'}\right] + \frac{\partial \phi'}{\partial x'} - \frac{F^2}{R_o^2}v' = 0, \tag{IV.5}$$

$$\frac{\partial v'}{\partial t'} + F\left[\frac{\partial (u'v')}{\partial x'} + \frac{\partial (v'w')}{\partial z'}\right] + u' = 0, \tag{IV.6}$$

$$\frac{\partial \theta'}{\partial t'} + F\left[\frac{\partial (u'\theta')}{\partial x'} + \frac{\partial (w'\theta')}{\partial z'}\right] + w' = 0, \tag{IV.7}$$

$$\frac{\partial u'}{\partial x'} + \frac{\partial w'}{\partial z'} = 0 \quad \text{and} \tag{IV.8}$$

$$\frac{\partial \phi'}{\partial z'} - \theta' = 0. \tag{IV.9}$$

Hydraulic jumps are formed through the action of the non-linear terms in Equations (IV.5), (IV.6) and (IV.7). Even when these terms are small ($F \ll 1$), they can produce a jump in a non-rotating system. If a hydraulic jump is to be prevented, the Coriolis term in (IV.5) must dominate the non-linear advective terms, which implies that

$$\frac{F^2}{R_o^2} \gg F. \tag{IV.10}$$

The curve dividing the jump region from the no-jump region should then have the form

$$F = A R_o^2 \tag{IV.11}$$

where the constant A should be appreciably larger than 1. Houghton's analytical curve corresponds to $A \simeq 6.5$; Williams and Hori [1970] found that A = 6.0 to 7.5 was in agreement with their numerical

solutions. As in Williams' and Hori's experiment, with A in the range 6.0 to 7.5, the above scale analysis does not apply for $F \sim 1$, since F is then greater than Ro.

Two regions in Ro are of interest when $F \sim 1$. If $Ro \sim 1$, all terms in Equations (IV.5), (IV.6) and (IV.7) are of the same order and a jump would be expected to form. However, when $Ro \ll 1$, the appropriate time scale is $T = f^{-1}$ and the v-scale is $V = U$. The non-dimensional equations then become

$$\frac{\partial u'}{\partial t'} + Ro\left[\frac{\partial (u'u')}{\partial x'} + \frac{\partial (u'w')}{\partial z'} + \frac{1}{F}\frac{\partial \phi'}{\partial x'}\right] - v' = 0, \qquad \text{(IV.12)}$$

$$\frac{\partial v'}{\partial t'} + Ro\left[\frac{\partial (u'v')}{\partial x'} + \frac{\partial (v'w')}{\partial z'}\right] + u' = 0 \quad \text{and} \qquad \text{(IV.13)}$$

$$\frac{\partial \Theta'}{\partial t'} + Ro\left[\frac{\partial (u'\Theta')}{\partial x'} + \frac{\partial (w'\Theta')}{\partial z'} + \frac{1}{F}w'\right] = 0 \qquad \text{(IV.14)}$$

along with Equations (IV.8) and (IV.9). If the terms in Ro are neglected, the resulting equations describe an inertial oscillation in u and v; the temperature field is independent of time.

The scale analysis indicates that, when F is small, the jump boundary is given by $F = ARo^2$, and that as F approaches 1, the boundary will be between Ro = 1.0 and Ro = 0.1. These results were tested by direct numerical integration of the basic equations.

V. INITIAL CONDITIONS

The initial x-averaged stability $\frac{\partial \bar{\theta}}{\partial z}$ is independent of z. A wave sinusoidal in x, the amplitude of which is directly dependent on the Froude number, is superimposed upon this basic state.

The initial fields for this experiment are given by the equations

$$u(x,0) = U \cos(kx) \left\{ \cos\left[\frac{\pi}{D}\left(z - \frac{D}{2}\right)\right] - \frac{2}{\pi} \right\},$$

$$v(x,0) = 0 \quad \text{and} \tag{V.1}$$

$$\theta(x,0) = -\frac{UN\theta_*}{g} \cos(kx) \sin\left[\frac{\pi}{D}\left(z - \frac{D}{2}\right)\right] - \frac{\partial \bar{\theta}}{\partial z}\left(z - \frac{D}{2}\right).$$

The constants which define the initial state have the following numerical values:

$$D = 3 \text{ km.},$$

$$\frac{\partial \bar{\theta}}{\partial z} = 4.0 \ ^\circ\text{K km.}^{-1} \quad \text{and} \tag{V.2}$$

$$\frac{g}{\theta_*} = 0.03269 \text{ m sec}^{-2} \ ^\circ\text{K}^{-1}.$$

The wavelength of the disturbance, L, is equal to 1,000 km.

After finite differences are introduced, it is necessary to adjust the values of u which are given by (V.1) in order that

$$w_k = -\sum_{j=\frac{1}{2}}^{j=K-\frac{1}{2}} \frac{\partial u_j}{\partial x}\left(z_{j+\frac{1}{2}} - z_{j-\frac{1}{2}}\right) = 0. \tag{V.3}$$

This merely states that the finite difference vertical velocity at the upper boundary must be zero.

The following initial conditions were also examined:

$$u(x,0) = U\cos(kx)\cos\left(\frac{\pi z}{D}\right),$$
$$v(x,0) = 0 \quad \text{and} \tag{V.4}$$
$$\theta(x,0) = -\frac{UN\theta_0}{g}\cos(kx)\sin\left(\frac{\pi z}{D}\right) + \frac{\partial\bar{\theta}}{\partial z}\left(\frac{D}{2} - z\right).$$

When f = 0 they lead to an exact finite amplitude wave solution which moves with the linear gravity wave speed. In this solution the non-linear terms in Equations (II. 7) and (II. 18) cancel out identically. In this case no jumps can occur although they were observed for $f \neq 0$.

VI. NUMERICAL SOLUTIONS

The numerical solutions are presented in non-dimensional form. The time for all results presented is given in units of the time scale, L/DN. Most of the results are for $F \sim 1$. Enough results are presented for $F < 1$ in order to determine the jump curve. This will provide a basis for comparison with the work done previously by Houghton [1969] and Williams and Hori [1970] in the one-layer, homogeneous system.

A quantity useful in the analysis of the jump criterion is defined as

$$d = \frac{(u_{max} - u_{min})}{L \left|\frac{\partial u}{\partial x}\right|_{max}} \qquad (VI.1)$$

The quantity $\frac{\partial u}{\partial x}$ is approximated by $(u_{i+1} - u_i)/\Delta x$. Here the subscripts max and min refer to the maximum and minimum overall points at a given time. The non-dimensional quantity d is a measure of the width of the zone through which u varies most rapidly. It will be an overestimate of this width when the values of u at the edges of the zone are not near u_{max} and u_{min}. However, if a discontinuity such as a pressure jump does occur, d must approach zero, since it is inversely proportional to the gradient of u.

Figure 2 shows the variation of d as a function of time (time unit L/DN) for F = 1.0 and Ro = ∞. Results are shown for three values of $\Delta x = 2\pi L/n$ corresponding to n = 20, 40 and 80. As can be seen, d decreases to a minimum at approximately DNt/L = 0.4.

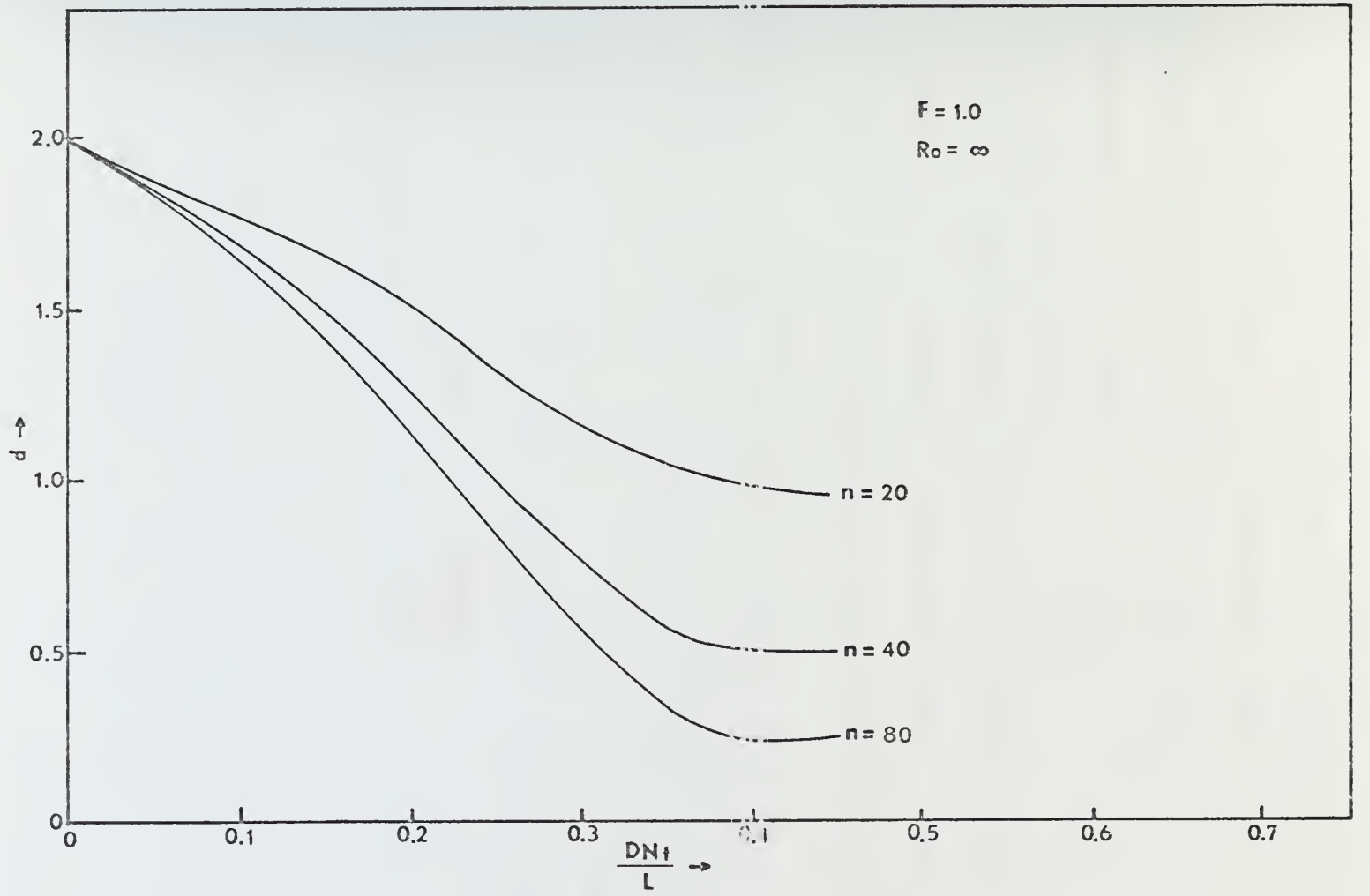

Fig. 2. The quantity d as a function of DNt/L for F=1.0 and Ro=∞. Each curve corresponds to a different value of x=2 L/n.

Detailed solutions are presented for three cases in which F = 1. In these numerical solutions $\Delta x = 2\pi L/n$, where n = 80. Figure 3 shows the time evolution of the non-dimensional variables $u' = u/U$ $v' = v/U$ and $\theta' = (\theta - \overline{\theta})/(UN\theta_o/g)$ [where $\overline{\theta}$ represents the horizontal average] for Ro = 1. The u and θ fields show that a hydraulic jump is forming at DNt/L = 0.37. The v field, which begins at zero, grows in opposite phase to the u and θ fields through the action of the Coriolis force. Once the v field is present, the Coriolis force will tend to reduce the amplitude of the u field while the amplitude of the θ field remains relatively unchanged throughout the period of integration. For this value of the Rossby number the Coriolis force was unable to prevent the formation of the hydraulic jump.

Figure 4 contains the evolution of the non-dimensional variables u', v' and θ' for Ro = 0.1. It appears that an inertial oscillation is present with the θ field remaining very nearly constant throughout the integration period. It was found that when the integration time was extended, though, the fields never were restored to the original as was shown for the one-layer, homogeneous case by Williams and Hori [1970].

The results for Ro = 0.35 are presented in Figure 5 using the same format as above. In this case there is no evidence of any reduction in the u field as the jump time is approached.

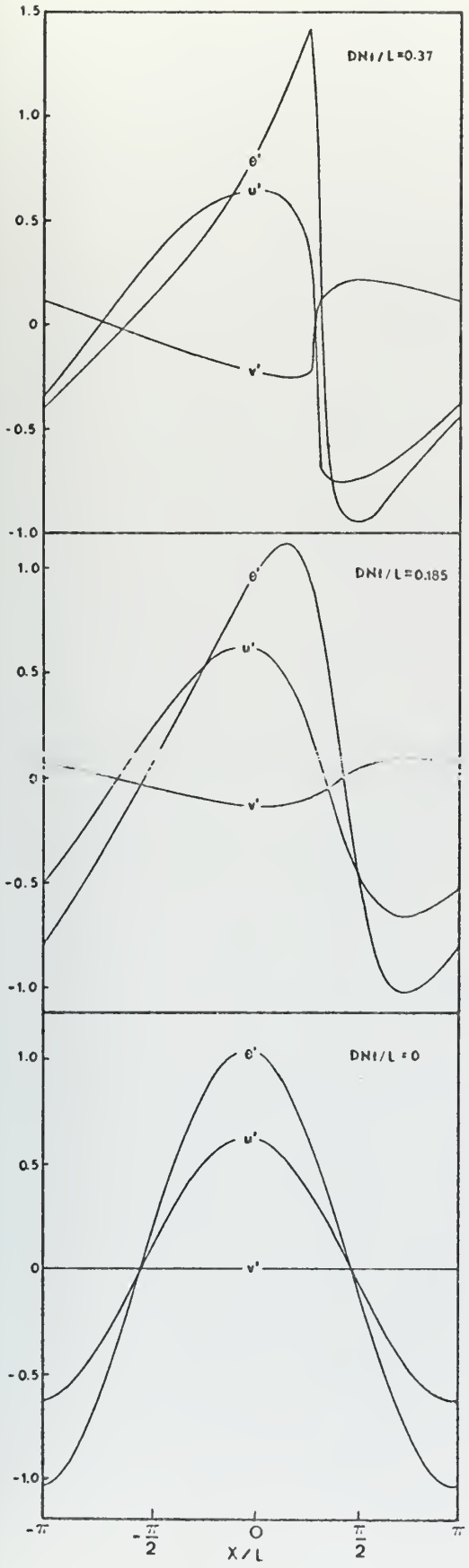

Fig. 3. The fields u', v' and θ' at various times for F=1.0 and Ro=1.0.

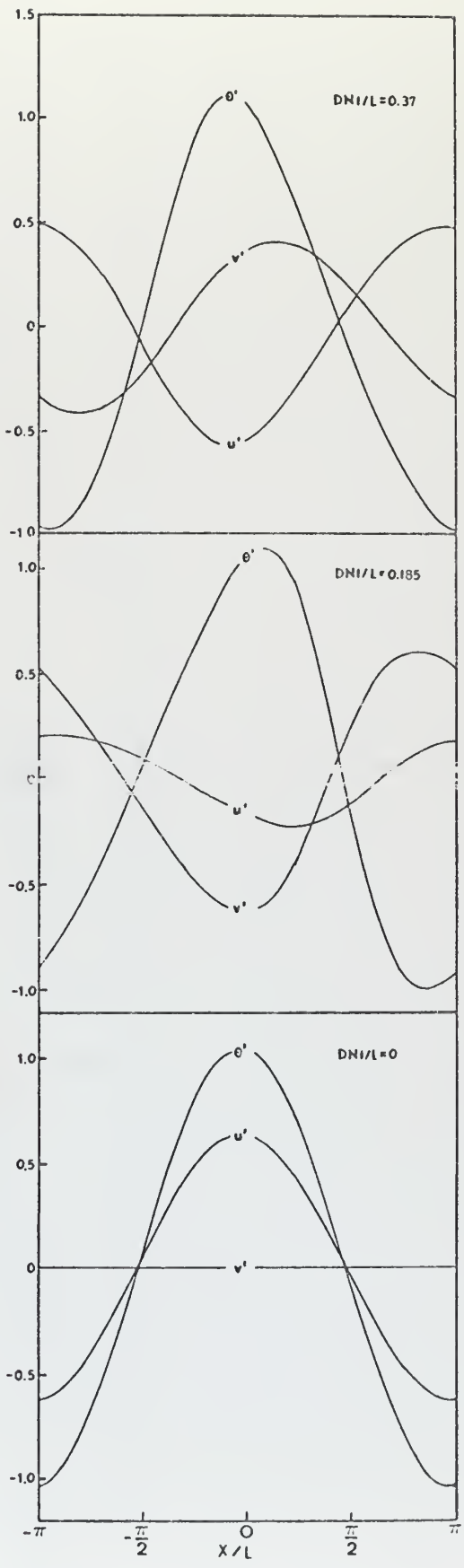

Fig. 4. The fields u', v' and θ' at various times for F=1.0 and Ro=0.1.

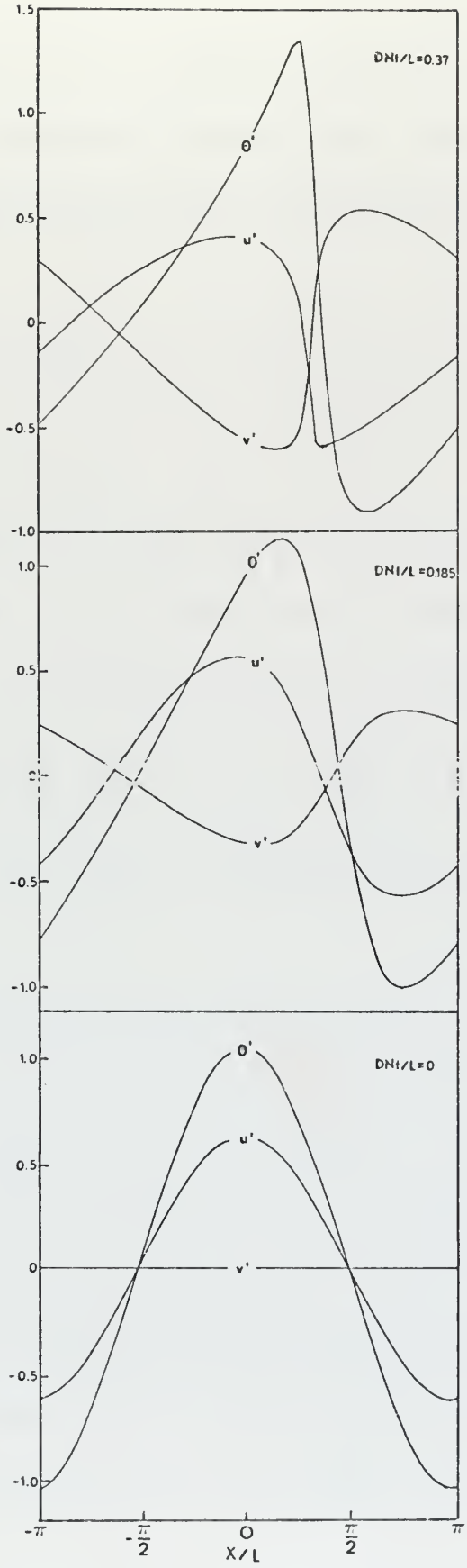

Fig. 5. The fields u', v' and θ' at various times for F=1.0 and Ro=0.35.

Results for F = 0.04 and Ro = 0.09 are contained in Figure 6 showing the evolution of u', v' and θ' for a typical jump case when $F \ll 1$. Figure 7 contains the evolution of the variables for F = 0.04 and Ro = 0.07 giving the results for a non-jump case when F is again much less than 1.

In Figure 8 and Figure 9 the results are presented for F = 0.3 and Ro = 0.3 and 0.1, respectively, showing the time evolution of u', v' and θ' when F is in the range 0.1 to 1.0.

The above figures are taken from the results of the lowest layer in the model. Figure 10 is included in order to show what is taking place in the other layers at time zero and at an approximate jump time. The case presented is for F = 1.0 and Ro = 1.0. As can be seen, only the lower half of the model is shown. This provides a picture of what is taking place in the most active of the layers in the model.

The d procedure was used to determine the curve separating the jump cases from the non-jump cases over the range F = 0.04 up to F = 1.0. These results are shown in Figure 11, with the logarithm of F plotted against the logarithm of Ro. The lines $F = 6.0Ro^2$ and $F = 7.5Ro^2$ are included for convenience. These results for Equation (IV.11), which was derived by scale analysis leading to the conclusion that A is in the range 6.0 to 7.5. This relation does not hold for $F \sim 1$, but this was to be expected since the analysis required that $F \lesssim Ro$.

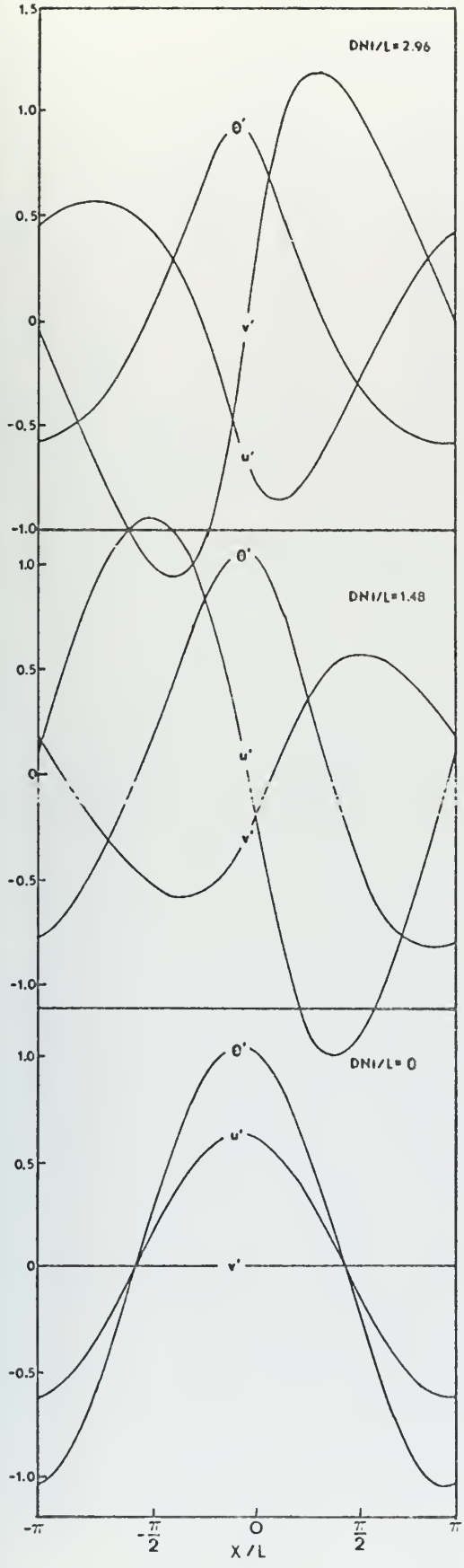

Fig. 6. The fields u', v' and θ' at various times for F=0.04 and Ro=0.09.

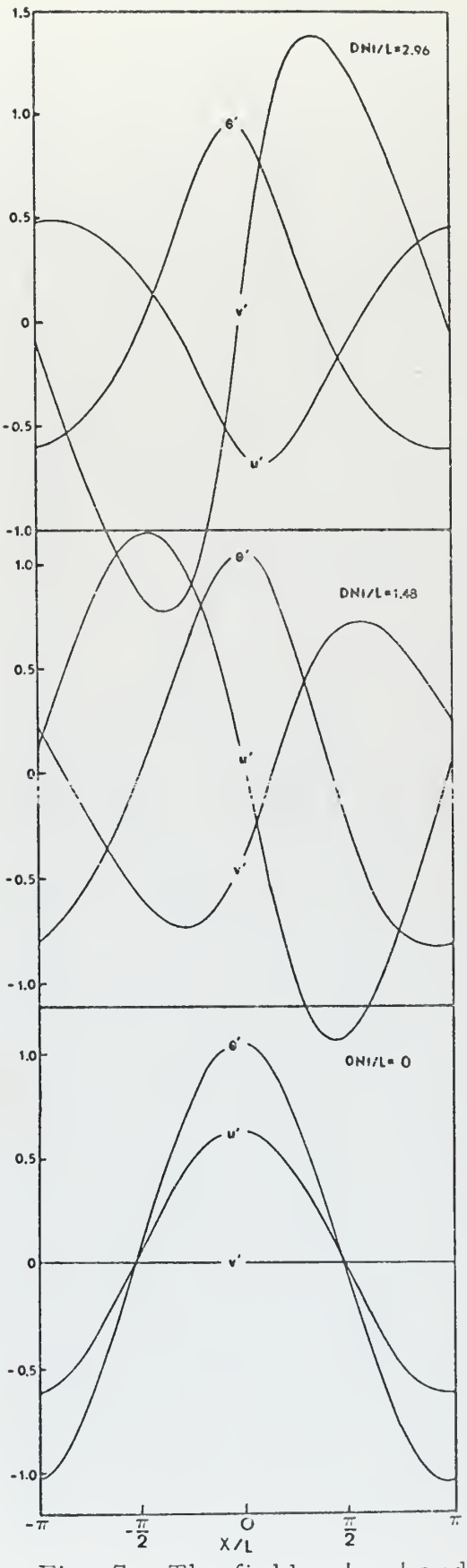

Fig. 7. The fields u', v' and θ at various times for F=0.04 and Ro=0.07.

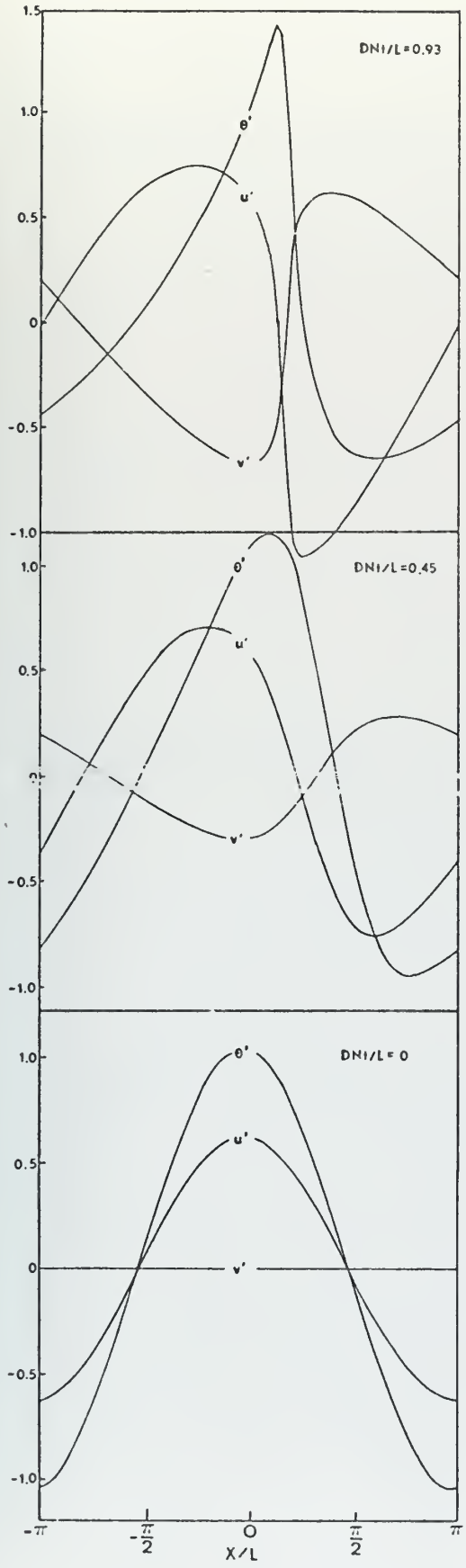

Fig. 8. The fields u', v' and θ' at various times for F=0.3 and Ro=0.3.

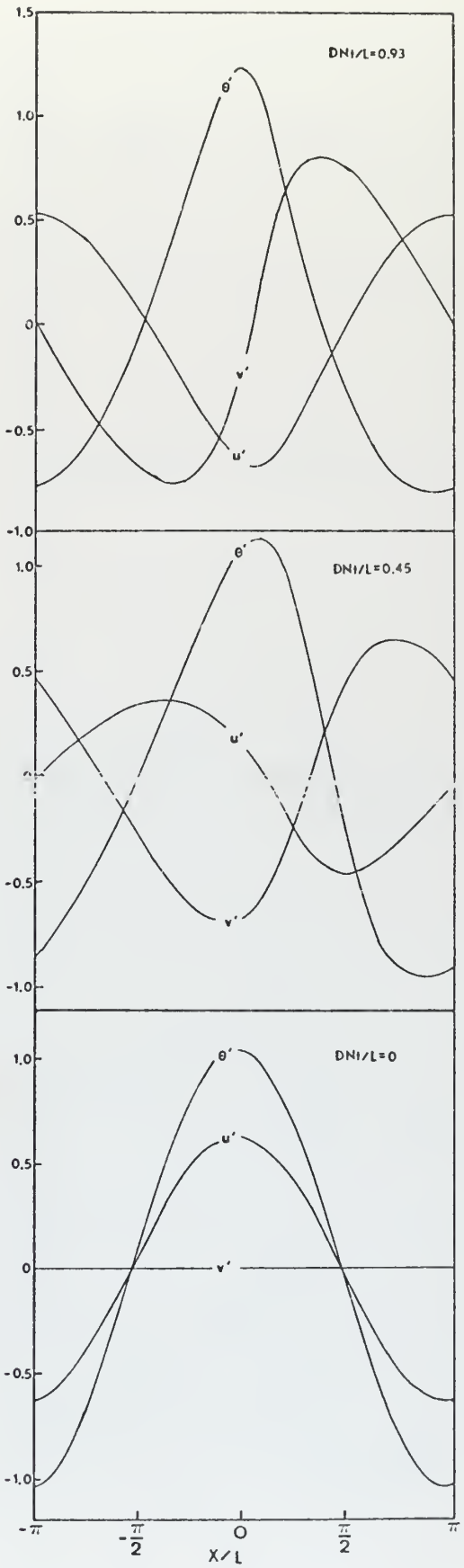

Fig. 9. The fields u', v' and θ' at various times for F=0.3 and Ro=0.1.

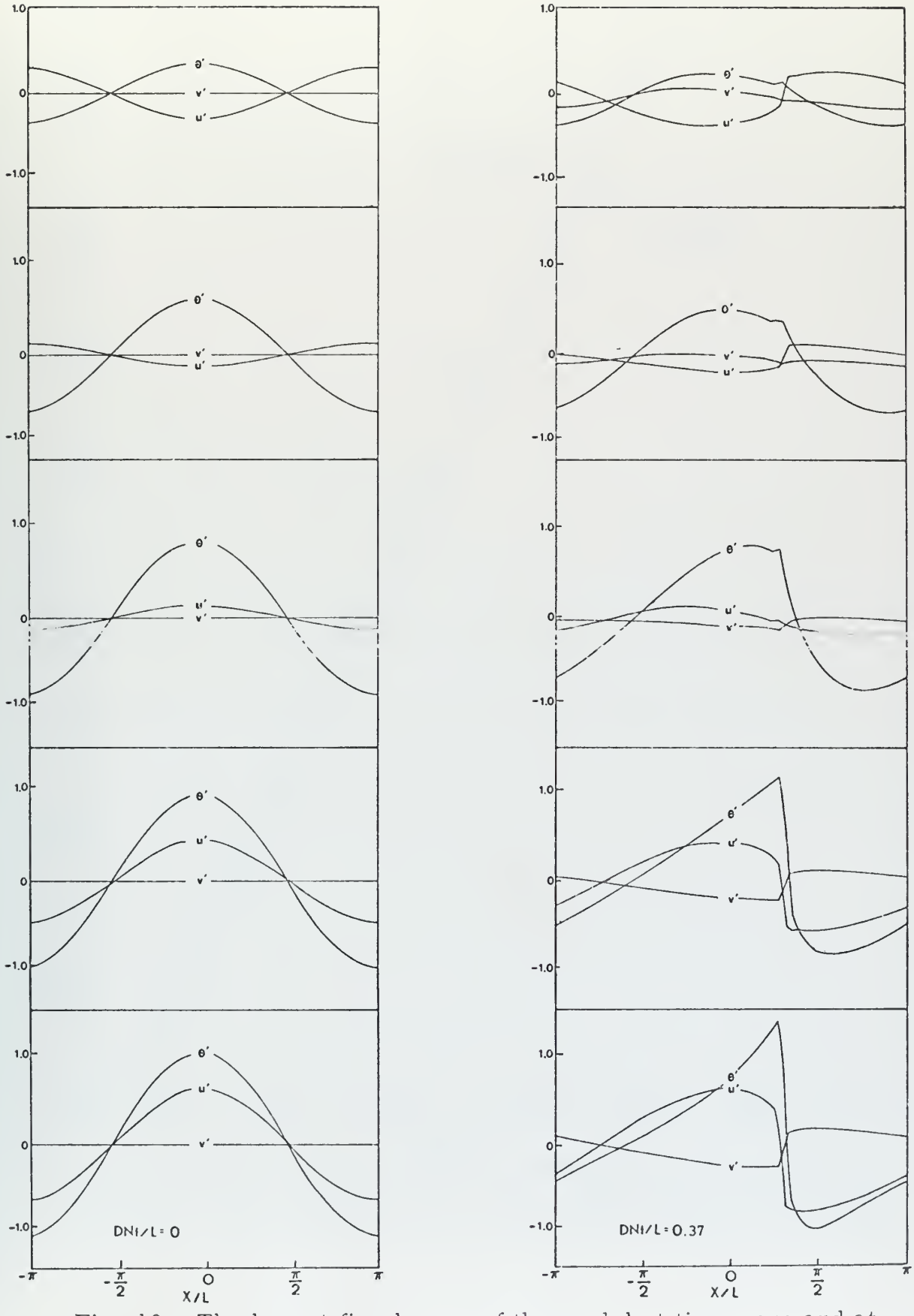

Fig. 10. The lowest five layers of the model at time zero and at approximate jump time for F=1.0 and Ro=1.0.

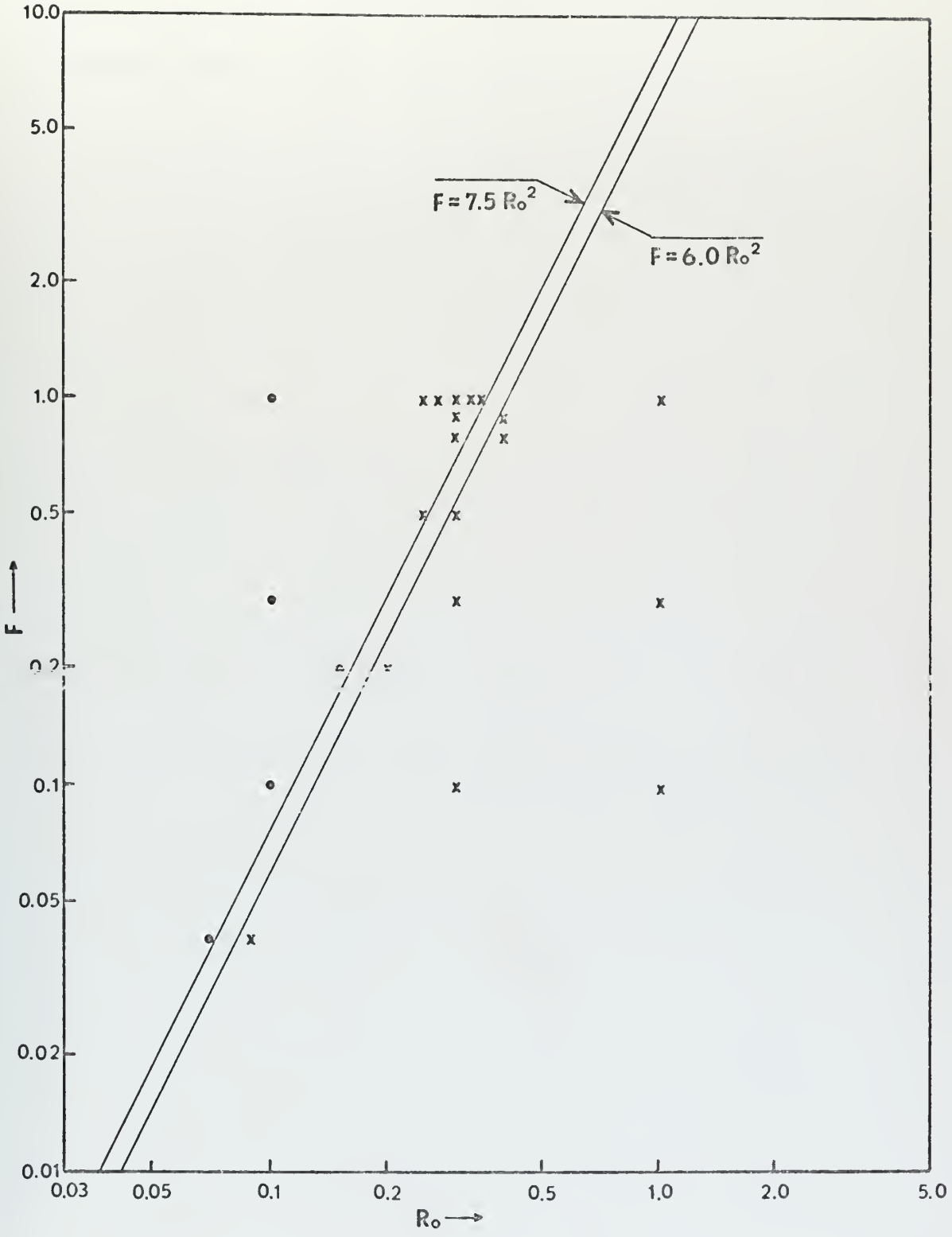

Fig. 11. Summary of jump-formation experiments with the logarithm of F plotted against the logarithm of Ro. The crosses indicate jump occurrence and the dots indicate cases where no jumps were found.

The non-jump solutions included in Figure 11 are determined over an integration time of L/DN.

VII. CONCLUSIONS AND RECOMMENDATIONS

The formation of hydraulic jumps in a rotating, continuously stratified fluid has been investigated. A scale analysis indicated that jump cases should be separated from non-jump cases by the curve $F = ARo^2$ in the F-Ro plane. The Rossby number Ro and the Froude number F were utilized as direct inputs to the equations and used as a means of determining the initial scales ($U = FDN$). It was determined that the results of this experiment (with F appropriately redefined) closely paralleled the results of Houghton [1969] and Williams and Hori [1970] in which one-layer, homogeneous fluids were studied. The numerical solutions of this experiment imply that A is in the range 6.0-7.5 and that the relation $F = ARo^2$ holds up to at least $F = 0.3$. Extrapolation to $F = 1.0$ showed jumps occurring for smaller values of Ro than were given by the above curve. Thus it can be seen that the jump criterion becomes more independent of F as $F = 1.0$ is approached.

This work should be extended to an atmosphere in which the jump region is bounded by a stable layer rather than a rigid plane as in this case. Such a study could require additional layers with further consideration given to layers of varying thickness. Further consideration should be given to moisture in future experiments.

LIST OF REFERENCES

1. Abdullah, A. J., 1966: The spiral bands of a hurricane: A possible dynamic explanation. J. Atmos. Sci., 23, 367-375.

2. Arakawa, A., 1966: Computational design for long-term numerical integration of the equations of fluid motion: Two-dimensional incompressible flow, 1. J. Comput. Phys., 1, 119-143.

3. Freeman, J. D., 1948: An analogy between the equatorial easterlies and supersonic gas flows. J. Meteor., 5, 138-146.

4. Gowans, G. K., 1969: Variation in thermal structure and geostrophic current between Alaska and Hawaii determined from synoptic space sections. Masters Thesis, Naval Postgraduate School, 74 pp.

5. Hinkelmann, K., 1959: Ein numerisches Experiment mit den primitiven Gleichungen. The Atmosphere and the Sea in Motion, New York, Rockefeiler Institute Press and the Oxford University Press, 486-500.

6. Houghton, D. D., and Kasahara, A., 1968: Nonlinear shallow fluid flow over an isolated ridge. Commun. Pure Appl. Math., 21, 1-23.

7. Houghton, D. D., 1969: Effect of rotation on the formulation of hydraulic jumps. J. Geophys. Res., 74, 1351-1360.

8. Lamb, H., 1945: Hydrodynamics, New York, Dover Publications, 738 pp.

9. Lilly, D. K., 1965: On the computational stability of numerical solutions of time-dependent non-linear geophysical fluid dynamics problems. Monthly Weather Review, 93, 11-26.

10. Lorenz, E. N., 1960: Energy and numerical weather prediction. Tellus, 12, 364-373.

11. Ogura, Y., and Charney, J. G., 1962: A numerical model of thermal convection in the atmosphere. Proc. Int. Symp. on Numer. Weather Predict., Tokyo, 431-452.

12. Ogura, Y., and Phillips, N. A., 1962: Scale analysis of deep and shallow convection in the atmosphere. J. Atmos. Sci., 19, 173-179.

13. Phillips, N. A., 1959: An example of nonlinear computational instability. The Atmosphere and the Sea in Motion, New York, Rockefeller Institute Press and Oxford University Press, 501-504.

14. Sasaki, Y., 1959: A numerical experiment for squall-line formation. J. Meteor., 16, 347-353.

15. Smagorinski, J., 1958: On the numerical integration of the primitive equations of motion for baroclinic flow in a closed region. Monthly Weather Review, 86, 457-466.

16. Tepper, J., 1952: The application of the hydraulic analogy to certain atmospheric flow problems. Weather Bur. Res. Pap. 35, 50 pp., U. S. Government Printing Office, Washington, D. C.

17. Williams, R. T., 1967: Atmospheric frontogenesis: A numerical experiment. J. Atmos. Sci., 24, 627-641.

18. Williams, R. T., and Hori, A. M., 1970: Formation of hydraulic jumps in a rotating system. J. Geophys. Res., 75, 2813-2821.

INITIAL DISTRIBUTION LIST

		No. Copies
1.	Defense Documentation Center Cameron Station Alexandria, Virginia 22314	2
2.	Library, Code 0212 Naval Postgraduate School Monterey, California 93940	2
3.	Department of Meteorology Naval Postgraduate School Monterey, California 93940	3
4.	Department of Oceanography Naval Postgraduate School Monterey, California 93940	1
5.	National Center for Atmospheric Research Box 1470 Boulder, Colorado 80302	1
6.	National Severe Storms Laboratory 1616 Halley Avenue Norman, Oklahoma 73069	1
7.	Dr. Joanne Simpson Experimental Meteorology Laboratory National Oceanographic and Atmospheric Administration Coral Gables, Florida 33124	1
8.	Dr. Y. Sasaki Department of Meteorology University of Oklahoma Norman, Oklahoma 73069	1
9.	Dr. N. A. Phillips 54-1422 M.I.T. Cambridge, Massachusetts 02139	1

10. Dr. M. G. Wurtele — 1
Department of Meteorology
UCLA
Los Angeles, California 90024

11. Dr. D. D. Houghton — 1
Department of Meteorology
University of Wisconsin
Madison, Wisconsin 53706

12. Dr. Jerry D. Mahlman — 1
Geophysical Fluid Dynamics Laboratory/NOAA
Princeton University
P. O. Box 308
Princeton, New Jersey 08540

13. Professor Noel E. Boston — 1
Department of Oceanography
Naval Postgraduate School
Monterey, California 93940

14. Professor Jerry L. Galt — 1
Department of Oceanography
Naval Postgraduate School
Monterey, California 93940

15. Professor Ronnie L. Alberty — 1
Department of Meteorology
Naval Postgraduate School
Monterey, California 93940

16. Professor Russell Elsberry — 1
Department of Meteorology
Naval Postgraduate School
Monterey, California 93940

17. Dr. George J. Haltiner — 1
Department of Meteorology
Naval Postgraduate School
Monterey, California 93940

18. Dr. Roger Terry Williams — 10
Department of Meteorology
Naval Postgraduate School
Monterey, California 93940

19. Lt. Robert Paul Kurth, USN
U. S. Naval Destroyer School
Newport, Rhode Island 02840 5

DOCUMENT CONTROL DATA - R & D

(Security classification of title, body of abstract and indexing annotation must be entered when the overall report is classified)

ORIGINATING ACTIVITY (Corporate author)
Naval Postgraduate School
Monterey, California 93940

2a. REPORT SECURITY CLASSIFICATION
Unclassified

2b. GROUP

REPORT TITLE
The Formation of Hydraulic Jumps in a Rotating, Continuously Stratified System

DESCRIPTIVE NOTES (Type of report and inclusive dates)
Master's Thesis; September 1971

AUTHOR(S) (First name, middle initial, last name)
Robert P. Kurth

REPORT DATE	7a. TOTAL NO. OF PAGES	7b. NO. OF REFS
September 1971	39	18

8a. CONTRACT OR GRANT NO.	9a. ORIGINATOR'S REPORT NUMBER(S)
b. PROJECT NO	
c.	9b. OTHER REPORT NO(S) (Any other numbers that may be assigned this report)
d.	

10. DISTRIBUTION STATEMENT
Approved for public release; distribution unlimited.

11. SUPPLEMENTARY NOTES	12. SPONSORING MILITARY ACTIVITY
	Naval Postgraduate School Monterey, California 93940

13. ABSTRACT

The formation of hydraulic jumps in a rotating, continuously stratified, Boussinesq fluid is investigated. A scale analysis indicates that jump-formation cases should be separated from non-jump cases by the curve $F = ARo^2$ where Ro and F are the initial Rossby and Froude numbers, respectively. Numerical solutions verify the curve up to $F = 0.3$ and show that A is in the range 6.0 to 7.5. The solutions for $F = 1.0$ are examined in considerable detail. The results of this paper extend the work of Houghton and Williams and Hori.

KEY WORDS	LINK A		LINK B		LINK C	
	ROLE	WT	ROLE	WT	ROLE	WT
Hydraulic Jumps						
Continuously Stratified Fluid						
Primative Equations						
Rotating Fluid						
Squall Line						

BINDERY

Thesis
K896
c.1

131671

Kurth
The formation of hydraulic jumps in a rotating, continuously stratified system.

BINDERY.

Thesis
K896
c.1

131671

Kurth
The formation of hydraulic jumps in a rotating, continuously stratified system.

thesK896
The formation of hydraulic jumps in a ro
3 2768 002 11578 4
DUDLEY KNOX LIBRARY